CHALMERS
UNIVERSITY OF TECHNOLOGY

Manufacturing Graphene-Encapsulated Copper Particles by Chemical Vapor Deposition in a Cold Wall Reactor

ChemPubSoc Europe

DOI: 10.1002/open.201800228

Open Access ChemistryOPEN Communications

Manufacturing Graphene-Encapsulated Copper Particles by Chemical Vapor Deposition in a Cold Wall Reactor

Shujing Chen,[a] Abdelhafid Zehri,[b] Qianlong Wang,[c] Guangjie Yuan,[a] Xiaohua Liu,[d] Nan Wang,[e] and Johan Liu*[a, b]

Functional fillers, such as Ag, are commonly employed for effectively improving the thermal or electrical conductivity in polymer composites. However, a disadvantage of such a strategy is that the cost and performance cannot be balanced simultaneously. Therefore, the drive to find a material with both a cost efficient fabrication process and excellent performance attracts intense research interest. In this work, inspired by the core–shell structure, we developed a facile manufacturing method to prepare graphene-encapsulated Cu nanoparticles (GCPs) through utilizing an improved chemical vapor deposition (CVD) system with a cold wall reactor. The obtained GCPs could retain their spherical shape and exhibited an outstanding thermal stability up to 179 °C. Owing to the superior thermal conductivity of graphene and excellent oxidation resistance of GCPs, the produced GCPs are practically used in a thermally conductive adhesive (TCA), which commonly consists of Ag as the functional filler. Measurement shows a substantial 74.6% improvement by partial replacement of Ag with GCPs.

Metallic particles have attracted tremendous research interests due to their unique electrical, thermal and mechanical properties, which may use as fillers in conductive ink, conductive adhesive or thermally conductive adhesive (TCA) to form electrical or thermal conductive path.[1–3] Fillers of noble metals, such as silver[2]and gold,[3] were intensively studied because of their promising electrical and thermal conductivities together with excellent anti-oxidation properties.[4] However, widespread applications of such metal particles are limited due to their high cost. Hence, more intensive research works are being carried out towards the synthesis of non-noble metal particles with decent electrical and thermal conductivity in combination with oxidation resistance.

The electrical and thermal conductivity of Cu are comparable to Ag, and the anti-electromigration ability of Cu is superior. In addition with the cost efficiency of Cu, this, all together, motivates Cu particles as an alternative approach to replace the noble metal particles in electrical conductive inks or TCAs. However, the challenge to apply bare fine Cu particles is that it will be easily oxidized to form Cu_2O within several hours when they are exposed to air at room temperature.[5] The formation of copper oxidation not only reduces the electrical conductivity, but also results in a degradation in thermal conductivity.[6] Therefore, anti-oxidation behaviors of Cu particles must be improved before they can be applied widely in practical applications.

Graphene, due to its extraordinary electrical conductivity,[7] high thermal conductivity[8] and chemical stability,[9] was selected as a promising candidate to encapsulate Cu particles to improve its oxidation resistance. For example, Luechinger et al adopted reducing flame synthesis to prepare Cu nanoparticles capped by few-layer graphene and applied them into conductive ink. It was confirmed that graphene encapsulation enhanced the overall thermal stability and electrical conductivity of Cu nanoparticles.[10] Wang et al reported a new method for the lager-scale fabrication of Cu nanoparticles encapsulated by multi-layer graphene via using a one-step metal-organic CVD at 600 °C. It was shown that GCPs exhibited excellent oxidation resistance.[11] Although these studies provided few methods to fabricate GCPs, the size and shape of GCPs were uncontrollable because they were fabricated by random coalescence of synthesized carbon/Cu nanoclusters originated from primary stage. As a result, graphene grown directly on spherical Cu particles by tube furnace has thus been considered. However, the attempted growth temperature of graphene on Cu using gaseous carbon sources in tube furnace was commonly close to 1000 °C,[12,13] which was higher than the melting point of Cu nanoparticles[14] and resulted in agglomeration. Therefore, optimization of graphene growth on Cu

[a] S. Chen, Dr. G. Yuan, Prof. J. Liu
SMIT Center
School of Mechatronic Engineering and Automation
Shanghai University
20 Chengzhong Rd., Shanghai 201800 (China)
E-mail: johan.liu@chalmers.se
[b] A. Zehri, Prof. J. Liu
Electronics Materials and Systems Laboratory
Department of Microtechnology and Nanoscience
Chalmers University of Technology
Kemivägen 9, SE-412 96 Göteborg (Sweden)
[c] Dr. Q. Wang
Shenzhen Institute of Advanced Graphene Application and Technology (SIAGAT)
Shenzhen 518106 (China)
[d] X. Liu
Shanghai Shang Da Ruihu Microsystem Integration Technology Co. Ltd.
Room 203, Building 2, No 1919, Fengxiang Road
Baoshan District, Shanghai 200444 (China)
[e] Dr. N. Wang
SHT Smart High Tech AB
Hugo Grauers Gatan 3A, SE-411 33 Göteborg (Sweden)

Supporting information for this article is available on the WWW under https://doi.org/10.1002/open.201800228

particles with lower synthetic temperature during encapsulation progress is imperative. Recently, Sun et al demonstrated that high quality graphene with controllable thickness was grown at temperature of 800 °C from different solid carbon sources, such as poly methyl methacrylate (PMMA) and small molecules (fluorene and sucrose).[15] Accordingly, Lee et al fabricated graphene-encapsulated Cu particles with diameters ranging from 40 nm to 1 μm by using PMMA as a solid carbon source, ascribed from PMMA converted to carbon layers at the temperature of 400 °C before being transformed into few layers graphene at the temperature of 800–900 °C, but Cu particles can remain spherical shape without agglomeration.[16] Nonetheless, solid PMMA must initially dissolve in organic solvent for uniform distribution on the surface of Cu particles, such as anisole,[15] dimethylformamide,[16] which are harmful for human's health and contaminative for environment. Additionally, Chen at al mixed PMMA powders with Cu powders by ball-milling method, and then put PMMA/Cu powders into tube furnace to synthesize graphene-Cu composite, but ball-milling deformed the morphology of Cu powders and led to agglomeration of Cu powders.[17] Therefore, it is a challenge to synthesize GCPs without generating agglomeration by using gaseous carbon source during deposition process.

In most studies, graphene was typically synthesized in tube furnace,[18–23] which is also known as the hot wall reactor because the heating source (usually a resistor or inductive foil) surrounds the outside of the quartz tube. However, temperature ramp-up and cool-down procedures are time consuming for graphene synthesis in hot wall reactor, due to its large heat capacity, which reduced the efficiency of fabrication.[21,22] In contrast, cold wall reactor contain a local heater of very low heat capacity, close to sample so that the effective reaction takes place in specific region refers to "target deposition", and brings advantages for effective lowering growth temperature, and shorting graphene growth time, which in return cuts down on overall cost and increases the yield.[24–26]

Herein, we, for the first time demonstrated a process to encapsulate Cu particles by few-layer graphene in a cold wall CVD reactor using gaseous carbon source. Since the growth temperature of graphene in a cold wall CVD reactor could be lowered to 775 °C, and graphene growth process performed directly on Cu particles, GCPs kept spherical morphologies after graphene growth. Raman analysis and high-resolution transmission electron microscope (HRTEM) confirmed few-layer graphene were successfully deposited on the Cu particles. Both the results of thermogravimetric integrated differential scanning calorimetry (TG-DSC) and X-ray diffraction (XRD) showed GCPs excellent thermal stability. In particular, prepared GCPs were also applied in TCA to demonstrate the thermal conductive feature practically.

Raman spectra were collected to illustrate an appropriate condition for graphene growth on the surface of Cu particles. Figure 1a and 1b demonstrate the Raman spectrum of GCPs fabricated by changing the H_2/CH_4 flow rate during procedure. Both Raman spectra show overlapped D and G peaks with high intensity situated at 1360 cm^{-1} and 1590 cm^{-1}, respectively. Broad peaks observed at 2300–3100 cm^{-1} represent 2D peaks.

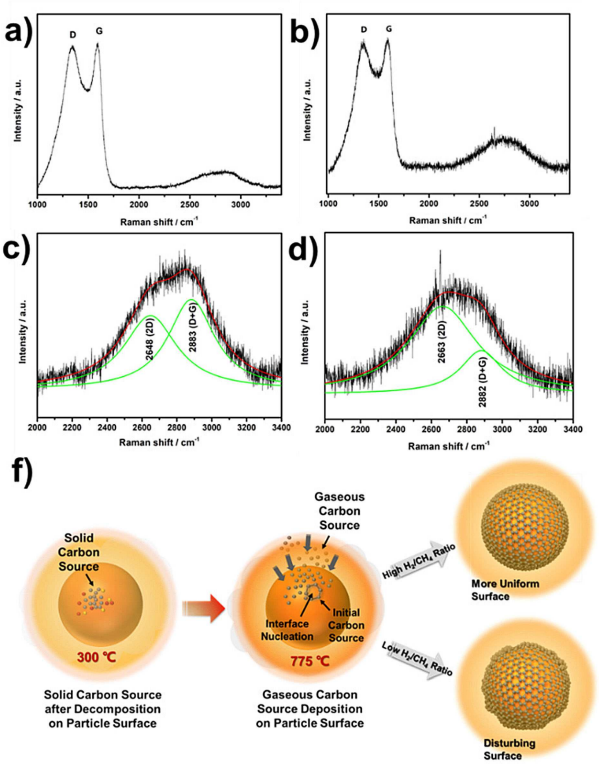

Figure 1. Raman spectra of GCPs synthesized by a low a) and high b) H_2/CH_4 ratio; c) and d) are the 2D regions fitted by Lorentzian profiles of (a) and (b), respectively; f) Schematic mechanism of manufacturing GCPs through cold wall CVD.

The strong defect D peak for both Raman spectrum may be explained by the formation of distorted hexagonal sp^2 hybridized carbon atoms in graphene,[27] together with strain-induced effects,[28,29] and finite particle-size effect.[11,30] These could be further explained by the high curvature of GCPs led to form stressed lattice structures within narrow domains.[16]

The peaks observed at 2300–3100 cm^{-1} in Figure 1 are broader than that observed for general multi-layer graphene, this may be attributed to nonplanar structure of graphene on Cu particles.[31] To further identify 2D peak, these broad peaks were fitted by Lorentz profiles, shown in Figure 1c and 1d. It could be found that the broad peaks are composed of 2D (at 2648 and 2663 cm^{-1}) and D + G (at 2883 and 2882 cm^{-1}) peaks. Generally, there is no D + G peak in planar graphene. However, it exists in nonplanar graphitic layers owing to strained structure.[31] Therefore, graphene synthesized on the surface of spherical Cu particles with high curvatures directly caused the presence of D + G peak of GCPs.

The relative intensity between the 2D and G peaks (I_{2D}/I_G) reflects the number of layers of graphene. I_{2D}/I_G ratio of GCPs fabricated by the high H_2/CH_4 ratio (15 : 4) was calculated at 0.2, which was higher than that (about 0.1) of GCPs fabricated by the low H_2/CH_4 ratio (3 : 1). HRTEM was carried out to characterize the number of layers of graphene, as shown in Figure S1 in Supporting Information. It can be seen that the number of graphene layers fabricated by the high H_2/CH_4 ratio is less than that of graphene layers fabricated by the low H_2/CH_4 ratio.

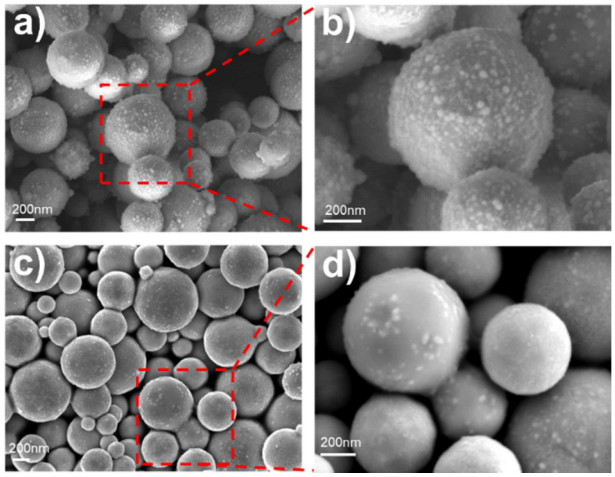

Figure 2. Low-magnification and high-magnification SEM images of Cu particles before (a, b) and after (c, d) graphene growth.

Hydrogen not only played the role of both carrier gas and reducing reagent, but also affected the speed of methane decomposition. Excessive hydrogen decreased methane decomposition, and then depressed the graphene growth speed.[25] Thus, within this work, the CH_4 flow rate of 8 sccm used for CVD was considered as preferred condition for few-layer graphene growth on Cu particles (Figure 1f).

Figure 2 represent the typical SEM images of Cu particles before and after graphene synthesis process at 775 °C. Pristine Cu particles with diverse diameters ranging from 200 nm to 550 nm are shown in Figure 2a and 2b. White spots on the surface of pristine Cu particles were characterized as sodium citrate, which is a surfactant to prevent Cu particles from agglomeration. After graphene growth at 775 °C, Cu particles retained their spherical shape and separate, as shown in Figure 2c. Cu particles did not agglomerate because of three reasons: initially, CVD process temperature here is lower than reported previously[16,25] and did not reach the melting temperature of Cu particles; secondly, sodium citrate containing carbon source decomposed after 300 °C, resulting in formation of carbon layers on the surface of Cu particles to prevent deformation of morphology. XPS data verified the complete decomposition of sodium citrate that was converted into carbon layers, as shown in Figure S2 in Supporting Information; finally, purchased pre-treated spherical Cu particles were used for graphene deposition. A filmy transparent layer may be visible on the surface of Cu particle (Figure 2d). However, there were some additional white spots attached on the surface of the observed graphene layer. EDS images indicate the white spots were composed of elementary carbon element (Figure S3 in Supporting Information). Therefore, additionally to methane as a gaseous carbon source during CVD process, sodium citrate served as a solid carbon source as well. The mechanism of fabricating GCPs is shown in Figure 1f. Due to uneven distribution of sodium citrate on the surface of Cu particles, the white spots are randomly spread on Cu surface.

The detailed morphological and structural characteristics of GCPs were starkly revealed by HRTEM, as shown in Figure 3. Figure 3a is wide angle view TEM of synthesized GCPs. It can be seen that Cu particles still retained its original shapes after graphene growth. The enlarged view (HRTEM) of Figure 3a is shown in Figure 3b. Noticeably, there are few ordered layer-like graphene shells with thickness of 1.5 nm–2.0 nm successfully grown on the surface of Cu particle. The interlayer distance between the graphene layers was measured at 0.33 nm, which is comparable to that of the reported value of 0.34 nm.[32] Figure 3c shows the HRTEM image of a single GCP. It is evident that the Cu particle is encapsulated by graphene layers and some redundant carbon, which agrees with the SEM result.

The thermal stability of the GCPs was investigated by TG-DSC in an oxygen atmosphere, as shown in Figure 4. There was a slight weight loss of 0.4% for GCPs at the beginning, attributed to the evaporation of physisorption water.[10,11] In addition, it could be seen that the initial oxidizing temperature for pristine Cu particles started at 133 °C, but was extended to 179 °C for GCPs, suggesting that the oxidation resistance of Cu particles was significantly improved by encapsulating with graphene. As shown in Figure 4b, the weight of particles increased slowly at 179 °C, rose rapidly at 253 °C, and climbed moderately at 374 °C. The TG-DSC results clearly indicate that the oxidation of GCPs by forming Cu_2O commenced at about 179 °C, and the combustion of graphene shells by reaction from C to CO_2 started at 253 °C. After that, Cu_2O was oxidized further to become CuO at 374 °C. The weight gain of pristine Cu particles was 24.61%, corresponding to the oxidation of Cu to CuO. However, the total mass gain of GCPs was 15.45% after the oxidation process. This implies that the weight content of graphene shells in GCPs is approximately 7.64%.

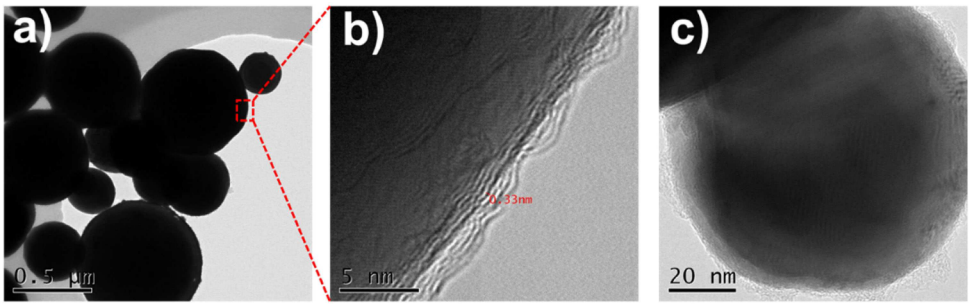

Figure 3. a) Low magnification TEM image of GCPs; b) The enlarged view of (a); c) HRTEM of a single GCP.

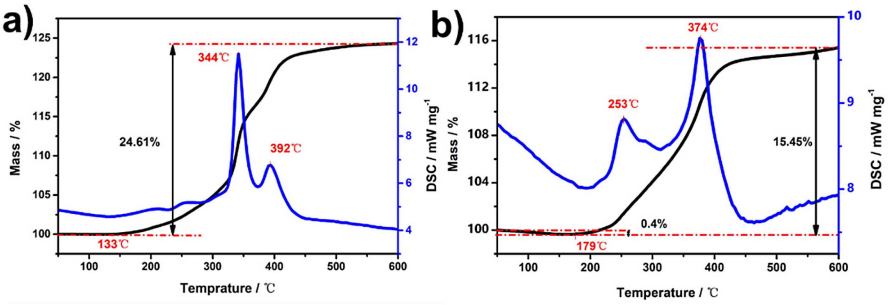

Figure 4. TG-DSC curves of pristine Cu particles (a) and GCPs (b).

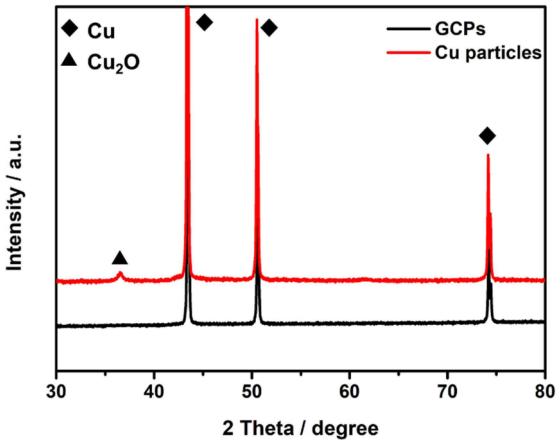

Figure 5. XRD patterns of pristine Cu particles and GCPs after annealing at 150 °C for 3 h.

To further investigate thermal stability, GCPs and pristine Cu particles were executed by thermally annealed under oxidation conditions at 150 °C for 3 hours. XRD phase analysis of both GCPs and pristine Cu particles were thereafter carried out as demonstrated in Figure 5. It is well known that fine Cu nanoparticles can be oxidized easily at room temperature within a few hours.[5] After thermal treatment, a clearly recognizable Cu_2O peak appeared at 36.6° for pristine Cu particles, besides Cu-related peaks at 43.4°(Cu(111)), 50.5°(Cu (200)) and 74.2°(Cu(220)). However, no sign of oxidation could be detected for GCPs. It can be inferred that graphene shells offered well protection for Cu particles from oxidation after annealing at 150 °C, which is in accordance with the results of TG-DSC. For additional aging test, GCPs were left to exposure in air at room temperature for more than 60 days, after that identical XRD diffraction results were obtained, revealing that GCPs were stable against oxidation, at least at the XRD detection level (Figure S4 in Supporting Information).

In a typical TCA, the active filler is usually a combination of flake Ag (75 wt%) and spherical nanosilver (nano-Ag) (5 wt%). The combination of different morphological fillers used in TCA system can increase the thermal conductive pathway, but also increase the thermal contact resistance.[33] Therefore, the mixing ratio of different morphological fillers in TCA that lead to high thermal conductivity is essential. In experiments, 5 wt% spherical nano-Ag is initially replaced by pristine spherical Cu particles and GCPs to compare thermal performances in TCAs, 75 wt% flake Ag remain unchanged. The measured thermal conductivity of these TCAs is presented in Figure 6a. It can be seen, by replacing spherical Ag with GCPs, the thermal performance of fabricated TCA is comparable to the original TCA with spherical Ag, but much better than the TCA with pristine spherical Cu particles. This can be explained by deposition with graphene layers on pristine Cu particles, the thermal conductivity is effectively improved. On the other hand, since TCA requires solidification at 150 °C for 1 hour, the untreated pristine Cu particles in TCA were inevitable to oxidize and thus reduced overall thermal conductivity. By treating with graphene layers resulted in GCPs are chemically inert, and thermal stable.

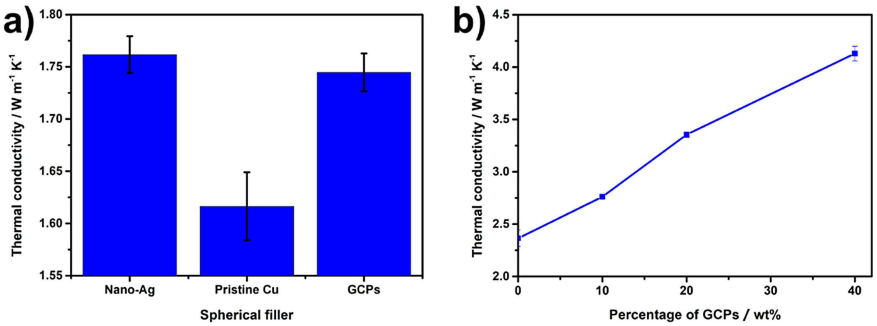

Figure 6. a) The effect of different spherical particles on thermal conductivity in TCA; b) The influence of weight distribution percentage of GCPs on thermal conductivity.

In order to further reduce overall cost and improve thermal conductive performance of TCA, flake Ag fillers were replaced partly by GCPs in TCA. For comparisons, four samples (85 wt% flake Ag, 75 wt% flake Ag + 10 wt% GCPs, 65 wt% flake Ag + 20 wt% GCPs, 45 wt% flake Ag + 40 wt% GCPs) were prepared. Figure 6b shows the effect of weight distribution percentage of GCPs on thermal conductivity when the total weight of metal fillers in TCA remained at 85 wt%. The thermal conductivity of TCA improved significantly with the increasing proportion of GCPs. When the weight of GCPs accounted for 40 wt%, the thermal conductivity of TCA rose to 4.13 $W m^{-1} K^{-1}$ (comparison of previously reported TCAs is listed in Table S1 in Supporting Information), which means 74.6% improvement over TCA filled by pure flake Ag. According to TG-DSC analysis, 40 wt% GCPs included 3 wt% graphene. Such improvement on thermal conductivity were accounted for the interaction between sub-micron Cu particles and graphene. Replacement of micron flake Ag with sub-micron GCPs resulted in increase of the thermally effective contact networks. Additionally, besides protecting Cu particles from oxidation, few-layer graphene dispersing uniformly in TCA provide low resistance for phonon path. This together with the superior thermal properties of graphene compared to Cu and Ag improves effectively the thermal conductivity.[34–36]

In summary, we developed a novel, efficient and facile process to fabricate GCPs without agglomeration through improved CVD process. A cold wall CVD method was firstly introduced in this work for fabricating few-layer graphene directly on spherical Cu particles by using gaseous carbon source. By adjusting gaseous flow rate, the deposited graphene layer on Cu particles can be optimized, and the outcome GCPs not only achieved integral encapsulation, but also remained their original spherical shapes without agglomeration. The cold wall CVD process offers the advantage on reducing the procedural temperature, as well as shortening processing time. GCPs processed by cold wall CVD possess excellent oxidative stability up to 179 °C, which resolves the critical problem of easy oxidation of fine Cu nanoparticles and opens up a wider application prospect. In addition, the superb thermal conductive property of processed GCPs allow for practical uses such as TCA. The measurements support the possibility of replacing nano-Ag and flake Ag by GCPs in TCA. In conclusion, owing to their unique physical features, GCPs are a strong candidate as functional filler materials for TCAs and conductive inks.

Experimental Section

Preparation of GCPs

200 nm-550 nm sodium citrate coated Cu particles with purity of 99.9% (from Aladdin Shanghai Biological Technology Co., Ltd) were used as catalyst for chemical vapor deposition of few-layer graphene. GCPs were synthesized in a cold wall CVD reactor (see Figure S6 in Supporting Information), as shown in Figure 7.

The Cu particles were put into Cu boat, and the boat was suspended above the graphite heater. A cover was put over the boat in order to prevent Cu particles to be blown away, resulting in contamination of chamber. The reactor chamber was then immediately pumped down to 0.1 mbar. The temperature of graphite heater was ramped up to 775 °C at a rate of 200 °C min^{-1} in a hydrogen/argon atmosphere and held constantly at 775 °C. When the temperature was stable, the Cu particles were annealed for additional 5 mins to remove any oxide completely and wait for sodium citrate decomposition. After that, CH_4, as a gaseous carbon source, was introduced into the chamber for initiating the graphene growth. Finally, the chamber temperature was decreased to below 150 °C before the particles were taken out when the growth was completed. In addition, two parallel experiments were carried out by changing synthetic conditions of CH_4 flow rate from 8 sccm to 10 sccm, in order to investigate the effects of the amount of CH_4 on formation of GCPs.

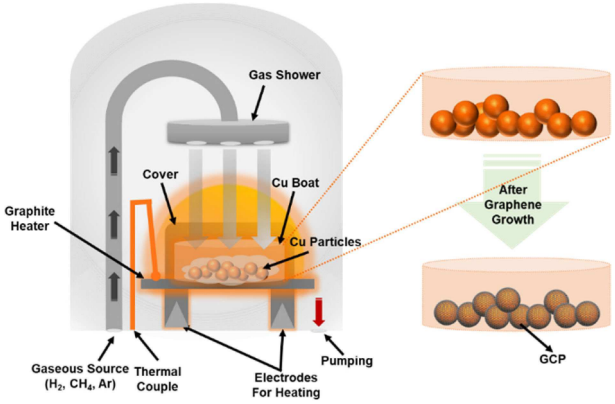

Figure 7. Schematic synthesis of GCPs in a cold wall CVD.

Characterization

After graphene growth, the particles were characterized by field emission scanning electron microscopy (SEM, ZEISS Merlin Compact), Raman Spectrometer (INVIA), X-ray Diffraction (XRD, 3 KW D/MAX2200 V PC) and transmission electron microscopy (TEM, FEI Tecnai G2 F20 S-TWIN). Thermal stability of the graphene-Cu particles was carried out in a thermogravimetric differential analyzer (Mettler Toledo) in flowed oxygen (flow rate: 40 mL min^{-1}) atmosphere at a heating rate of 10 °C min^{-1}. XRD was used to verify the anti-oxidation feature of prepared GCPs after annealing at 150 °C for 3 hours. Moreover, the thermal conductivity of TCA with GCPs was measured by using Xenon NanoFlash (NETZSCH LFA 447).

Acknowledgements

The authors acknowledge financial support from the Ministry of Science and Technology of China with the contract No: 2017YFB0406000. We thank for the financial support from the Swedish Foundation for Strategic Research (SSF) under contract No. GMT14-0045 and SE13-0061 and from the Production Area of Advance at Chalmers University of Technology, Sweden.

Conflict of Interest

A patent application has been filed.

Keywords: cold wall reactor · copper particles · graphene · oxidation resistance · thermal conductivity

[1] H. J. Jiang, K. S. Moon, J. X. Lu, C. P. Wong, *J. Electron. Mater.* **2005**, *34*, 1432.
[2] S. Magdassi, A. Bassa, Y. Vinetsky, A. Kamyshny, *Chem. Mater.* **2003**, *15*, 2208.
[3] B. T. Anto, S. Sivaramakrishnan, L. L. Chua, P. K. H. Ho, *Adv. Funct. Mater.* **2010**, *20*, 296.
[4] H. S. Kim, J.-u. Jang, H. Lee, S. Y. Kim, S. H. Kim, J. Kim, Y. C. Jung, B. J. Yang, *Adv. Eng. Mater.* **2018**.
[5] X. M. Liu, Y. C. Zhou, *J. Mater. Res.* **2005**, *20*, 2371.
[6] S. Magdassi, M. Grouchko, A. Kamyshny, *Materials* **2010**, *3*, 4626.
[7] A. K. Geim, K. S. Novoselov, *Nat. Mater.* **2007**, *6*, 183.
[8] N. Wang, M. K. Samani, H. Li, L. Dong, Z. Zhang, P. Su, S. Chen, J. Chen, S. Huang, G. Yuan, X. Xu, B. Li, K. Leifer, L. Ye, J. Liu, *Small* **2018**, e1801346.
[9] S. S. Chen, L. Brown, M. Levendorf, W. W. Cai, S. Y. Ju, J. Edgeworth, X. S. Li, C. W. Magnuson, A. Velamakanni, R. D. Piner, J. Y. Kang, J. Park, R. S. Ruoff, *ACS Nano* **2011**, *5*, 1321.
[10] N. A. Luechinger, E. K. Athanassiou, W. J. Stark, *Nanotechnology* **2008**, *19*.
[11] S. L. Wang, X. L. Huang, Y. H. He, H. Huang, Y. Q. Wu, L. Z. Hou, X. L. Liu, T. M. Yang, J. Zou, B. Y. Huang, *Carbon* **2012**, *50, 2119*.
[12] H. C. Lee, H. Bong, M. S. Yoo, M. Jo, K. Cho, *Small* **2018**, *14*.
[13] T. S. Kol'tsova, T. V. Larionova, N. N. Shusharina, O. V. Tolochko, *Tech. Phys.* **2015**, *60*, 1214.
[14] C. Mattevi, H. Kim, M. Chhowalla, *J. Mater. Chem.* **2011**, *21*, 3324.
[15] Z. Z. Sun, Z. Yan, J. Yao, E. Beitler, Y. Zhu, J. M. Tour, *Nature* **2010**, *468*, 549.
[16] S. Lee, J. Hong, J. H. Koo, H. Lee, S. Lee, T. Choi, H. Jung, B. Koo, J. Park, H. Kim, Y. W. Kim, T. Lee, *ACS Appl. Mater. Interfaces* **2013**, *5*, 2432.
[17] Y. K. Chen, X. Zhang, E. Z. Liu, C. N. He, Y. J. Han, Q. Y. Li, P. Nash, N. Q. Zhao, *J. Alloys Compd.* **2016**, *688*, 69.
[18] Q. F. Liu, Y. P. Gong, J. S. Wilt, R. Sakidja, J. Wu, *Carbon* **2015**, *93*, 199.
[19] W. Liu, S. Kraemer, D. Sarkar, H. Li, P. M. Ajayan, K. Banerjeet, *Chem. Mater.* **2014**, *26*, 907.
[20] H. B. Sun, J. Wu, Y. Han, J. Y. Wang, F. Q. Song, J. G. Wan, *J. Phys. Chem. C* **2014**, *118*, 14655.
[21] L. X. Liu, H. L. Zhou, R. Cheng, W. J. Yu, Y. Liu, Y. Chen, J. Shaw, X. Zhong, Y. Huang, X. F. Duan, *ACS Nano* **2012**, *6*, 8241.
[22] P. Zhao, S. Kim, X. Chen, E. Einarsson, M. Wang, Y. N. Song, H. T. Wang, S. Chiashi, R. Xiang, S. Maruyama, *ACS Nano* **2014**, *8*, 11631.
[23] X. Liu, L. Fu, N. Liu, T. Gao, Y. F. Zhang, L. Liao, Z. F. Liu, *J. Phys. Chem. C* **2011**, *115*, 11976.
[24] W. Mu, S. X. Sun, D. Jiang, Y. F. Fu, M. Edwards, Y. Zhang, K. Jeppson, J. Liu, *J. Electron. Mater.* **2015**, *44*, 2898.
[25] W. Mu, Y. F. Fu, S. X. Sun, M. Edwards, L. L. Ye, K. Jeppson, J. Liu, *Chem. Eng. J.* **2016**, *304*, 106.
[26] S. Das, J. Drucker, *Nanotechnology* **2017**, *28*, 105601.
[27] A. C. Ferrari, J. C. Meyer, V. Scardaci, C. Casiraghi, M. Lazzeri, F. Mauri, S. Piscanec, D. Jiang, K. S. Novoselov, S. Roth, A. K. Geim, *Phys. Rev. Lett.* **2006**, *97*.
[28] Z. Chen, G. S. Hong, H. L. Wang, K. Welsher, S. M. Tabakman, S. P. Sherlock, J. T. Robinson, Y. Y. Liang, H. J. Dai, *ACS Nano* **2012**, *6*, 1094.
[29] Y. J. Xiong, Y. Xie, Z. Q. Li, C. Z. Wub, R. Zhang, *Chem. Commun.* **2003**, *904*.
[30] M. A. Pimenta, G. Dresselhaus, M. S. Dresselhaus, L. G. Cancado, A. Jorio, R. Saito, *Phys. Chem. Chem. Phys.* **2007**, *9*, 1276.
[31] P. H. Tan, S. Dimovski, Y. Gogotsi, *Philos T Roy Soc A* **2004**, *362*, 2289.
[32] M. Ishigami, J. H. Chen, W. G. Cullen, M. S. Fuhrer, E. D. Williams, *Nano Lett.* **2007**, *7*, 1643.
[33] H. W. Chiang, C. L. Chung, L. C. Chen, Y. Li, C. P. Wong, S. L. Fu, *J. Adhes. Sci. Technol.* **2005**, *19*, 565.
[34] O. Eksik, S. F. Bartolucci, T. Gupta, H. Fard, T. Borca-Tasciuc, N. Koratkar, *Carbon* **2016**, *101*, 239.
[35] Y. X. Fu, Z. X. He, D. C. Mo, S. S. Lu, *Int. J. Therm. Sci.* **2014**, *86*, 276.
[36] M. Inagaki, Y. Kaburagi, Y. Hishiyama, *Adv. Eng. Mater.* **2014**, *16*, 494.

Manuscript received: October 23, 2018
Revised manuscript received: December 4, 2018
Version of record online: ■■, ■■■